Available online at www.sciencedirect.com
SCIENCE DIRECT®
Journal of Catalysis 221 (2004) 413–420
JOURNAL OF CATALYSIS
www.elsevier.com/locate/jcat

Deactivation of the water–gas-shift activity of Pd/ceria by Mo

S. Zhao, T. Luo, and R.J. Gorte *

Department of Chemical Engineering, University of Pennsylvania, Philadelphia, PA 19104, USA

Received 14 July 2003; revised 28 August 2003; accepted 3 September 2003

Abstract

The effect of surface Mo on the water–gas-shift (WGS) activity of Pd/ceria was studied. A series of 1 wt% Pd catalysts, with varying Mo content, were prepared from supports obtained by aqueous impregnation of $(NH_4)_2MoO_4$ onto ceria. Rates were found to decrease linearly with Mo coverage up to 1.8 Mo/nm^2 and were 10% of that on Pd/ceria after the addition of this amount of Mo. TPD studies with 2-propanol on the Mo-containing ceria demonstrate a relationship between the loss of WGS activity and the ceria sites that decompose the alcohol to propene and water. FTIR measurements suggest that Mo ions exchange with surface hydroxyls on ceria and that carbonates are not formed on ceria surfaces that have 1.8 Mo/nm^2. The results from CO–O_2 pulse measurements suggest that the Mo-containing surface is much harder to reduce than pure ceria. Raman spectra of the Mo-containing ceria show features associated with molybdena only for Mo coverages greater than 1.8 Mo/nm^2. The implications of these results for understanding WGS activity on Pd/ceria are discussed.

Keywords: Ceria; Pd; Molybdena; Water–gas-shift reaction; 2-Propanol

1. Introduction

Ceria-supported, precious metals have been getting increased attention as water–gas-shift catalysts for fuel cell fuel processors [1–3]. In addition to showing significantly higher reaction rates than traditional Cu/ZnO catalysts under some conditions relevant to fuel processors, the ceria-based catalysts are much less sensitive toward start-up/shut-down cycles and are not pyrrophoric. While questions about their long-term stability remain [4], it is not clear how large this problem really is [3] and there is indication that it can be resolved in any case [5]. Finally, the reaction is almost zeroth order in CO on ceria-supported precious metals, due to the redox mechanism in which the metal remains saturated in CO to low CO pressures [6,7]. This low reaction order is favorable for fuel cell applications since it allows for high rates at low CO pressures.

One of the most intriguing scientific aspects of ceria catalysis is that its properties depend strongly on pretreatment conditions and on doping with other oxides. For example, when precious metals are supported on ceria films that have been calcined at temperatures below 1073 K, the catalytic properties of the material are consistent with facile transfer of oxygen from ceria to the metal [8,9]. The oxidation of Pd films by an underlying ceria–zirconia support was also observed spectroscopically to occur at moderate temperatures [10]. However, when pure ceria is calcined to higher temperatures, it becomes more difficult to reduce, resulting in a significant decrease in the activity of ceria-supported metals [11,12]. Consistent with this, CeO_2 single crystals, which by definition have been heated to high temperatures during their preparation, are difficult to reduce except by very harsh treatments such as ion sputtering [12,13]. (Note that ordered ceria films-grown-stabilized zirconia crystals are highly reducible and should not be considered in this category [14].) Deactivation of the oxygen storage capacity of ceria by high temperatures in automotive applications is well known, and it is necessary to stabilize the reducibility of ceria for that application by mixing it with zirconia [15].

In a recent study of water–gas-shift (WGS) catalysis over Pd/ceria [16], it was shown that the addition of only 5 mol% of MoO_x to the surface of ceria decreased the reaction rates at 473 K by an order of magnitude without changing the activation energy for the reaction. This result is interesting for a number of reasons. First, given that molybdena has interesting redox properties, one might expect that it would promote the WGS reaction rather than poison it. Second, the small quantities required to significantly reduce the reaction rate

* Corresponding author.
E-mail address: gorte@seas.upenn.edu (R.J. Gorte).

0021-9517/$ – see front matter
doi:10.1016/j.jcat.2003.09.004

suggest that Mo is very efficient at poisoning the reaction and that determining how the Mo poisons the reaction might provide insights into the reaction mechanism and the nature of the active sites.

In the present study, we have examined the poisoning of ceria by Mo more carefully to try to understand how the two oxides interact. We will show that Mo ions react with surface hydroxyls on ceria and that the reducibility of the ceria surface is effectively poisoned by coverages less than 2.0 Mo/nm^2.

2. Experimental

The catalysts used in this study were prepared from ceria powder that was synthesized by decomposition of $Ce(NO_3)_3 \cdot 6H_2O$ (Alfa Aesar, 99.5%) in air at 873 K. This support was then modified by aqueous impregnation with varying amounts of $(NH_4)_2MoO_4$ (Alfa Aesar, 99.997%), dried at 383 K overnight, and finally calcined in air at 873 K for 4 h. After preparing the support, Pd was added by wet impregnation using aqueous solutions of $Pd(NH_3)_4(NO_3)_2$ (Aldrich, 99.99%). Following impregnation of the Pd salt, the catalysts were dried at 383 K and calcined at 873 K. The Pd content was maintained at 1 wt% in all the Pd-containing catalysts used in this study. A complete list of the Mo–ceria supports is given in Table 1. All of the Mo loadings are listed as weight percent Mo.

A wide range of techniques was used to characterize the samples. First, surface areas were determined from BET isotherms with N_2 on each of the supports after outgassing at 623 K. Next, the nature of the surface sites on each of the supports was probed using simultaneous temperature-programmed-desorption (TPD) and thermogravimetric-analysis (TGA) measurements of isopropanol, as has been described elsewhere [17]. Briefly, approximately 70 mg of sample was placed in the sample pan of a Cahn 2000 microbalance, heated in vacuum ($\sim 10^{-7}$ Torr), and then exposed to 5 Torr of isopropanol at room temperature. After evacuation for 1 h, the sample temperature was ramped at 20 K/min while monitoring the sample weight and the partial pressures above the sample with an Inficon residual-gas analyzer.

Table 1
BET surface area of supports used in this study

Catalyst	BET surface area (m^2/g)	Mo surface site density ($\mu mol/m^2$)	Mo surface site density (Mo atoms/nm^2)
Ceria	61 (63)	0	0
0.25 wt% Mo–ceria	59	0.44	0.26
0.5 wt% Mo–ceria	58	0.90	0.54
0.75 wt% Mo–ceria	56 (55)	1.41	0.85
1 wt% Mo–ceria	54	1.93	1.16
1.25 wt% Mo–ceria	44 (42)	2.97	1.79
1.5 wt% Mo–ceria	37	4.22	2.64
2 wt% Mo–ceria	34	6.14	3.70
4 wt% Mo–ceria	32	13.0	7.84
MoO_3	9	–	–

The FTIR spectra were recorded using a Mattson Galaxy FTIR instrument with a diffuse–reflectance attachment, Collector II, provided by Spectra-Tech Inc. This system allowed spectroscopic measurements to be performed between room temperature and 773 K, with flowing gases of any desired composition. The samples were placed inside the chamber without packing or dilution. Spectra were taken in He after oxidizing the samples at 673 K for 30 min in flowing O_2 and after exposure to 25 Torr CO at 673 K for 30 min. A total of 256 scans were accumulated in each measurement at a resolution 2 cm^{-1}. Raman spectra were recorded using a Renishaw Raman microspectrometer Ramascope 1000 and a diode laser (780-nm excitation wavelength, 12 W/cm^2). The samples were examined in air at room temperature, with no additional treatment beyond the calcination used in the sample preparation.

The WGS rates were measured in a $\frac{1}{4}$-inch, Pyrex tubular reactor operating at atmospheric pressure, using ~ 100 mg of sample. Water was introduced by saturation of a He carrier gas flowing through deionized water. The partial pressures of CO, H_2O, and He were controlled by adjusting the relative flow rates of each component. In this study, all of the reaction measurements were collected with partial pressures for CO and H_2O of 25 Torr. All the reaction rates were measured under differential conditions, with less than 10% conversion of the limiting reagent. Before analyzing the products, we always allowed the reaction to run for at least 30 min to avoid potential transients associated with catalyst conditioning. Under the reaction conditions used in this study, rates were completely stable with time. The reaction products were measured using a gas chromatograph (SRI8610C) equipped with a Hayesep Q column and a TCD detector.

The transient-pulse experiments were performed on a system that has been described previously [18]. Computer-controlled switching valves allowed the composition of reactants admitted to a tubular reactor to undergo step changes. The product gases leaving the reactor could be analyzed by an on-line quadruple mass spectrometer. Integration of the partial pressures as a function of time allowed accurate determination of the amounts of oxygen that could be added or removed at different temperatures. The carrier gas was pure He, with relatively dilute amounts of CO (5% in He), O_2 (7% in He), and H_2O (2% in He) added in the pulses. The amount of catalyst used in the pulse studies was 1.0 g.

3. Results

Table 1 gives the surface areas of the ceria and Mo-modified ceria supports used in this study, as determined by BET analysis. (The surface areas given in parentheses in the table are values that were measured a second time to demonstrate the reproducibility of the values.) The surface areas decrease slowly with Mo content up to approximately

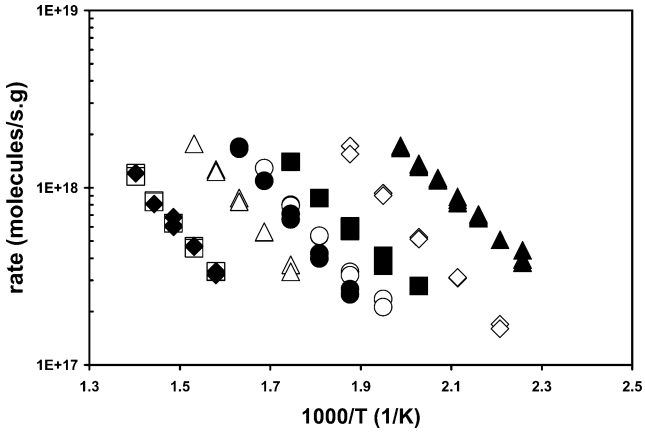

Fig. 1. Differential rates for the WGS reaction on 1 wt% Pd/ceria (▲), 1 wt% Pd/0.5 wt% Mo–ceria (◇), 1 wt% Pd/1 wt% Mo–ceria (■), 1 wt% Pd/1.25 wt% Mo–ceria (○), 1 wt% Pd/1.5 wt% Mo–ceria (●), 1 wt% Pd/2 wt% Mo–ceria (△), 1 wt% Pd/4 wt% Mo–ceria (□), 1 wt% Pd/MoO_3 (◆).

1 wt%, but then appear to decrease much more rapidly with additional Mo. The decrease in surface area is approximately 12% after the addition of 1 wt% Mo but 44% after addition of 2 wt% Mo. To determine whether the Mo addition decreases surface area by blocking access to micropores or by causing a growth in the ceria crystallite size, X-ray diffraction (XRD) measurements were performed on samples with 0, 1.0, and 2.0 wt% Mo. The average CeO_2 crystallite size was calculated to be 6.0, 6.8, and 9.0 nm on these three samples based on Scherrer analysis. While the specific surface areas for these crystallite sizes should be much higher than we observe (spherical particles, 6.0 nm in diameter, should result in a specific surface area of $\sim 140\ m^2/g$), the increase in crystallite size clearly follows the decrease in surface area, indicating that the addition of MoO_3 to the surface probably assists in the sintering of ceria crystallites. One should expect that the additional processing steps required to add Mo to the ceria could increase the crystallite size and this could account for the increase to 6.8 nm upon addition of 1 wt% Mo. However, the significant increase observed for the 2 wt% Mo sample suggests that Mo also enhances sintering of ceria.

The effect of added Mo on the water–gas-shift rates are shown in Fig. 1 and Table 2 for differential conversions with 25 Torr of CO and 25 Torr of H_2O. In each case, the rates were measured after adding 1 wt% Pd to the supports listed in Table 1. Since we were only able to maintain differential reaction conditions over a limited range of rates, the most active samples were those that achieved these rates at the lowest temperatures. To compare rates at a common temperature in Table 2, it was necessary to extrapolate the rates on some samples using the activation energies determined from a linear regression of the data in Fig. 1. Clearly, the Pd/ceria catalyst without adding Mo showed the highest rates, with Mo-containing samples exhibiting rates that decreased with increasing Mo content. Rates on the Pd/4 wt% Mo–ceria sample were indistinguishable from rates on Pd/MoO_3. It is

Table 2
Differential reaction rates and activation energies for the water–gas-shift reaction on Mo-modified Pd/ceria catalysts

Catalyst	Rate at 553 K ($\times 10^{17}$ molecules/(s g))	Relative rate	Activation energy (kJ/mol)
1 wt% Pd/ceria	44.5[a]	1	47
1 wt% Pd/0.5 wt% Mo–ceria	24.7[a]	0.56	57
1 wt% Pd/1 wt% Mo–ceria	8.72	0.20	55
1 wt% Pd/1.25 wt% Mo–ceria	5.33	0.12	53
1 wt% Pd/1.5 wt% Mo–ceria	4.11	0.09	64
1 wt% Pd/2 wt% Mo–ceria	2.20[a]	0.05	63
1 wt% Pd/4 wt% Mo–ceria	0.66[a]	0.01	58
1 wt% Pd/MoO_3	0.66[a]	0.01	58

[a] These values are extrapolated to 553 K from the Arrhenius plots in Fig. 1.

also interesting to consider that the addition of 1.25 wt% Mo decreased the WGS rate by almost a factor of 10. This coverage of Mo corresponds to 1.8×10^{18} Mo/m^2, a specific coverage that is less than one would normally associate with a monolayer capable of blocking the surface of ceria.

Because alcohols should interact in a very different manner with MoO_3 and ceria, TPD-TGA measurements were performed with 2-propanol adsorption to provide information on how Mo modifies the surface properties of ceria. Fig. 2 shows TPD-TGA curves obtained after a brief exposure to 2-propanol vapor for pure ceria and for ceria with 1 wt% Mo. In Fig. 2a, the result for pure ceria, the initial alcohol coverage after evacuation was ~ 210 μmol/g, 2.1×10^{18} molecules/m^2. A significant fraction of this desorbs as 2-propanol ($m/e = 45$) and a smaller amount as acetone ($m/e = 43$) below 500 K. Most of the remaining 2-propanol reacts to propene ($m/e = 41$) and water, with propene leaving the sample between 500 and 625 K. (Water desorbs over a wide temperature range, making it difficult to monitor.) By using the TGA results, the amount of propene leaving the pure ceria sample was calculated to be 9.3×10^{17} molecules/m^2. Following the addition of 1 wt% Mo, the TPD-TGA curves appear very different. The quantity of 2-propanol remaining on the surface decreases significantly, to 140 μmol/g (1.6×10^{18} molecules/m^2, 76% of that adsorbed on pure ceria). Even more important, the amount of propene leaving the sample between 500 and 625 K decreases to 1.5×10^{17} molecules/m^2, a quantity that is only 16% of that formed on pure ceria. Re-exposure of 2-propanol to both ceria and Mo-modified ceria to 2-propanol resulted in essentially identical TPD-TGA results, without the need for oxidation of the samples, demonstrating that the samples were not modified by the experiment and that no residue remained on the surface from the previous exposure to 2-propanol.

TPD-TGA experiments with 2-propanol were performed on the other samples listed in Table 1, and the major change observed with Mo loading was in the amount of propene formed between 500 and 625 K. The amounts of propene formed during TPD-TGA of 2-propanol are given in Table 3

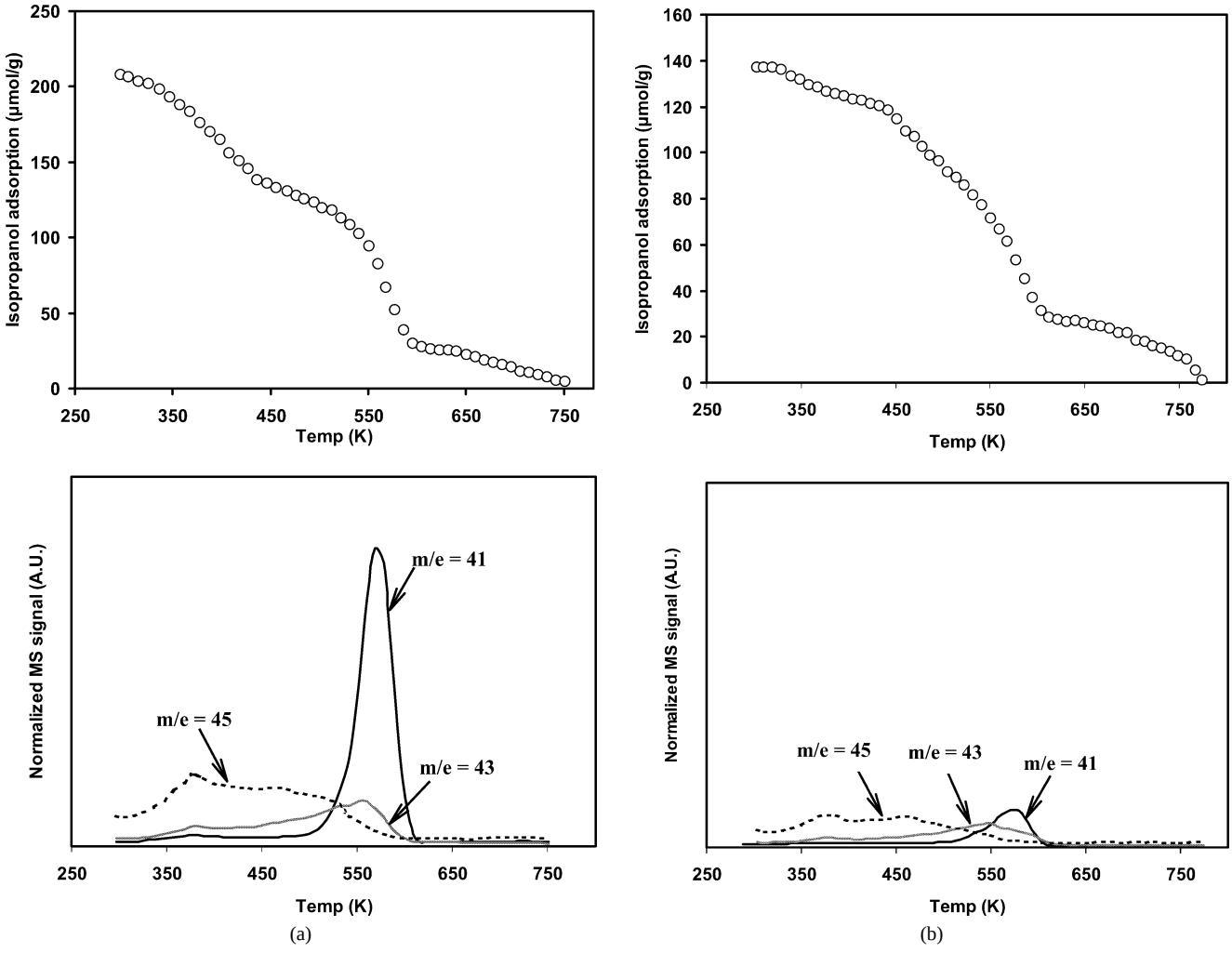

Fig. 2. TPD-TGA curves for 2-propanol from (a) pure ceria and (b) 1 wt% Mo on ceria.

Table 3
2-Propanol uptake at room temperature and propene production in the temperature range 500–625 K

Catalyst	2-Propanol (μmol/g)	Propene production from 500 to 625 K ($\times 10^{18}$ molecules/g)	($\times 10^{17}$ molecules/m^2)
Ceria	208	57.0	9.3
0.25 wt% Mo–ceria	193	47.0	8.0
0.5 wt% Mo–ceria	177	37.0	6.4
0.75 wt% Mo–ceria	155	29.0	5.2
0.85 wt% Mo–ceria	147	9.0	–
1 wt% Mo–ceria	137	7.4	1.5
1.25 wt% Mo–ceria	118	< 0.1	–
1.5 wt% Mo–ceria	82	< 0.1	–
2 wt% Mo–ceria	65	< 0.1	–
4 wt% Mo–ceria	56	< 0.1	–
MoO_3	0	< 0.1	–

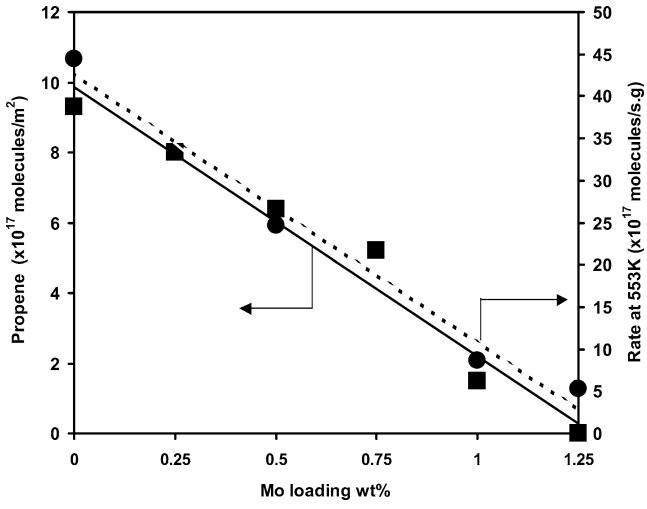

Fig. 3. WGS reaction rates and propene production from TPD-TGA shown as a function of Mo loading. The WGS reaction rates at 553 K for different samples are shown as the circles, and the propene production in the temperature range 500 to 625 K from the 2-propanol TPD are shown as squares.

and plotted along with the WGS activity of the Pd-loaded catalysts in Fig. 3. The plot in Fig. 3 shows that the amount of propene formed by desorption of 2-propanol decreases almost linearly with the Mo content to a coverage of approx-

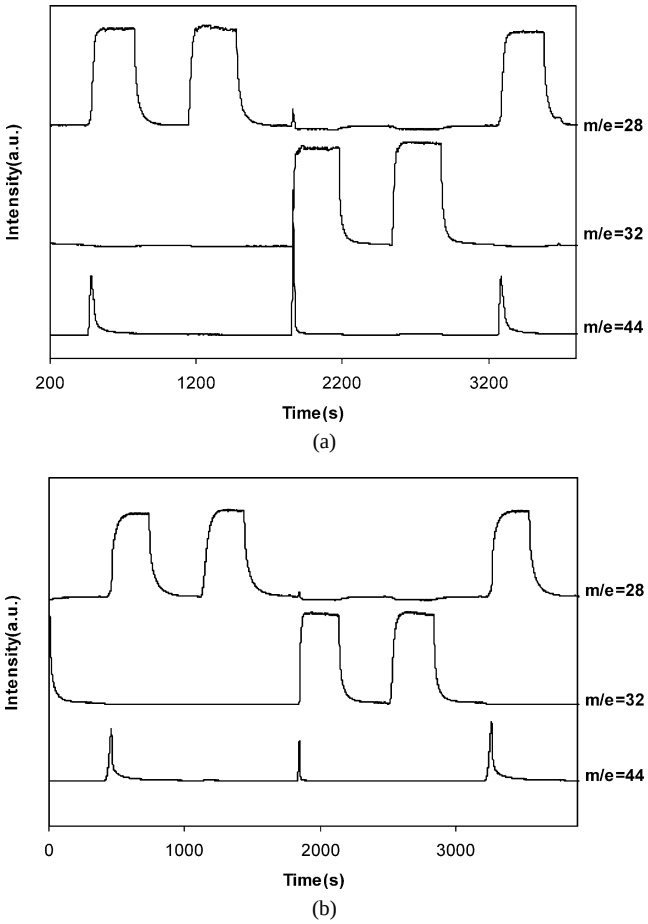

Fig. 4. Pulse measurements on (a) 1 wt% Pd/ceria and (b) 1 wt% Pd/1 wt% Mo–ceria at 473 K. The data are for two pulses of CO ($m/e = 28$), followed by two pulses of O_2 ($m/e = 32$) and another CO. Formation of CO_2 ($m/e = 44$ and 28) is observed in all of the pulses.

imately 1.25 wt% Mo. Fig. 3 also shows that decreases in the WGS activity follow the TPD-TGA results almost exactly, implying that there is a correspondence between the two measurements. Based on the initial slopes of the lines for the WGS rates and the TPD-TGA results, 1.25 wt% Mo completely modifies the ceria surface.

To understand how Mo modifies the properties of ceria, CO–O_2 pulse studies were performed on catalysts with 1 wt% Pd on the ceria and 1 wt% Mo–ceria samples. Typical data for these two catalysts are shown in Fig. 4 for measurements at 473 K. For Pd/ceria (Fig. 4a), the initial CO pulse ($m/e = 28$) partially reduces the catalyst, forming 135 μmol/g CO_2 ($m/e = 44$ and 28). A subsequent pulse of CO on this reduced catalyst forms only negligible amounts of additional CO_2. Similar to what was reported in previous studies [7,18], more CO_2 is formed (115 μmol/g) in a sharp peak when the reduced sample is exposed to O_2 ($m/e = 32$). A fraction of the CO_2 formed during the O_2 pulse is likely due to reaction of oxygen with CO adsorbed on the Pd; however, the amount of CO_2 that is formed is too large to be explained by this reaction. In a previous study, it was shown that the CO_2 formed during the O_2 pulse is due to decomposition of a surface carbonate that is stable only with Ce^{3+}, an assignment that was confirmed by FTIR measurements [7]. The data for Pd on 1 wt% Mo–ceria, shown in Fig. 4b, have a similar appearance to that for Pd/ceria, with the exception that much less CO_2 (38 μmol/g) is formed during the O_2 pulse. As we will demonstrate shortly when the FTIR results are presented, the surface carbonate is not formed on the Mo-containing sample and most of this CO_2 is likely formed by reaction of O_2 with CO adsorbed on Pd.

Table 4
Oxygen atom transferred in the CO–O_2 pulse

Catalyst	Oxygen transferred under different temperature (μmol/g)					
	323 K	373 K	433 K	473 K	523 K	573 K
1% Pd/ceria	86	135	215	250	340	435
1% Pd/ 1 wt% Mo–ceria	83	97	97	160	255	385

Data like that in Fig. 4 allow the quantification of oxygen transfer on the two catalysts and this information is given in Table 4 as a function of temperature. We interpret the data as showing that Mo prevents oxidation and reduction of the ceria surface. At 323 K, the total oxygen transfer (i.e., the sum of CO_2 formed in the CO and O_2 pulses) was approximately 85 μmol/g on both samples, with roughly the same amounts of CO_2 formed during the CO and O_2 pulses. This value can be explained by adsorption and reaction of O_2 and CO on Pd. A 1 wt% Pd corresponds to 100 μmol/g. Assuming a Pd dispersion of 40%, it is reasonable that approximately 40 μmol/g of CO_2 is formed by reduction of adsorbed oxygen with CO and that 40 μmol/g of CO would remain on the surface after the CO pulse, to be oxidized in the subsequent O_2 pulse. On the Pd/ceria catalyst, the amount of transferred oxygen increases dramatically with temperature, to 135 μmol/g at 373 K and 215 μmol/g at 423 K. The maximum amount of oxygen that can be transferred by the Pd, even assuming 100% dispersion and complete oxidation of the metal, is 200 μmol/g, implying that the ceria is also being oxidized and reduced. The amount of transferred oxygen increases with temperature as more of the oxygen from the bulk is available. With Pd on 1 wt% Mo–ceria, the amount of oxygen transfer is constant until 473 K, implying that oxygen transfer from the support is negligible below this temperature. At the highest temperatures, where oxygen from bulk ceria is accessible, the differences between the two catalysts do not appear as dramatic.

The diffuse–reflectance, FTIR measurements shown in Fig. 5 provide insights into how Mo reacts with the ceria surface. The spectra in this figure were measured after oxidation in pure O_2 at 673 K to remove a majority of carbonates, after which the samples were cooled in flowing He. For pure ceria, the peaks observed at 3740, 3700, and 3635 cm^{-1} have been assigned to stretches of unidentate, bidentate, and tridentate hydroxyls [19], while the broad band centered at 3510 cm^{-1} is believed to correspond to adsorbed water. The unidentate and bidentate hydroxyls are almost completely removed by

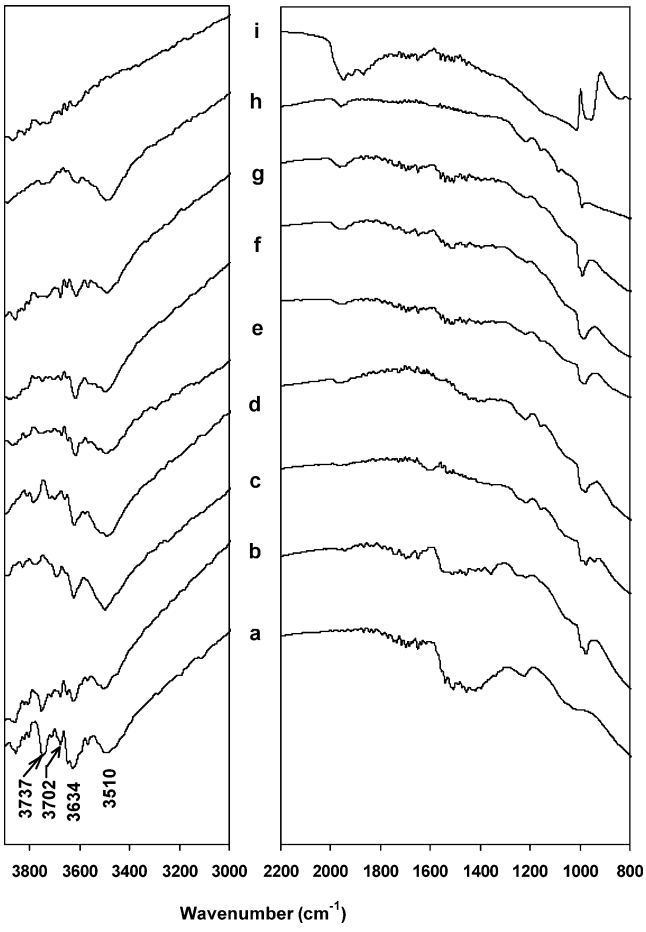

Fig. 5. FTIR data for Mo-containing samples after oxidation in O_2 at 673 K: (a) ceria, (b) 0.5 wt% Mo–ceria, (c) 0.75 wt% Mo–ceria, (d) 1 wt% Mo–ceria, (e) 1.25 wt% Mo–ceria, (f) 1.5 wt% Mo–ceria, (g) 2 wt% Mo–ceria, (h) 4 wt% Mo–ceria, and (i) MoO_3.

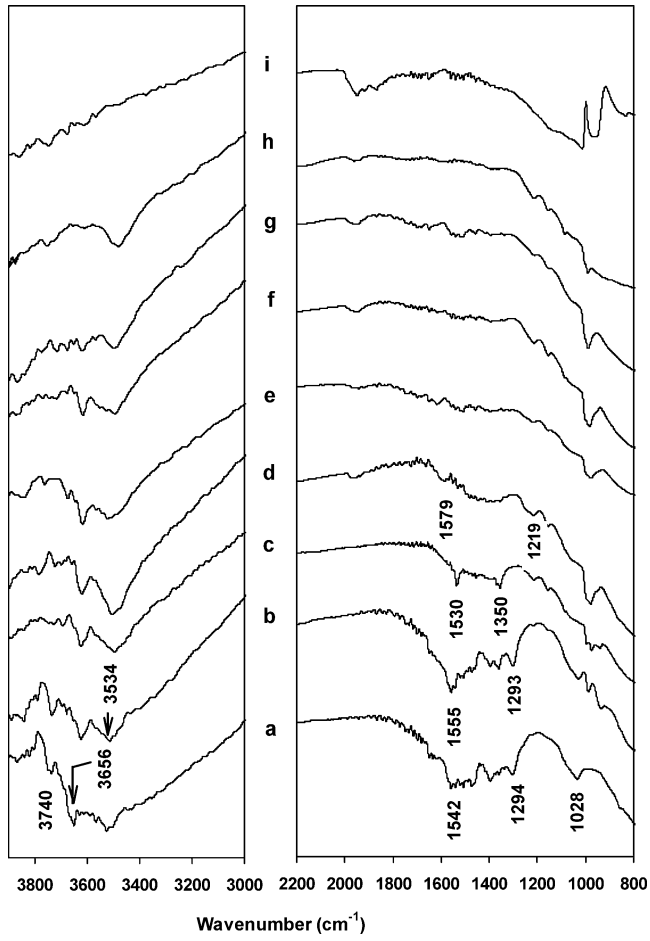

Fig. 6. FTIR data for Mo-containing samples after exposure to 25 Torr CO at 673 K: (a) ceria, (b) 0.5 wt% Mo–ceria, (c) 0.75 wt% Mo–ceria, (d) 1 wt% Mo–ceria, (e) 1.25 wt% Mo–ceria, (f) 1.5 wt% Mo–ceria, (g) 2 wt% Mo–ceria, (h) 4 wt% Mo–ceria, and (i) MoO_3.

the addition of 1.25 wt% Mo (spectrum e), suggesting that the Mo ions react with hydroxyl sites on the ceria surface. Molecular water is found on all of the Mo-containing surfaces, with the exception of pure MoO_3.

Fig. 6 shows the FTIR spectra obtained on the same samples after they had been heated in CO at 673 K. The peaks in the range from 1200 to 1600 cm^{-1} on pure ceria are an indication of carbonate formation. The intensities of the carbonate bands decrease with the addition of Mo and are essentially completely removed by the addition of 1.25 wt% Mo (spectrum e). It is also interesting to note that the hydroxyl bands appear unchanged by the formation of the carbonates.

Finally, Raman spectra were measured on selected Mo-containing samples, with the results shown in Fig. 7. It is noteworthy that no new features were observed on the sample containing 1 wt% Mo (spectrum b), over that observed on pure ceria (spectrum a). One observes new bands at 632, 818, and 975 cm^{-1} on the sample with 1.25 wt% Mo (spectrum c); and these grow in intensity on the sample with 4 wt% Mo (spectrum d). The new bands are almost certainly associated with a surface form of MoO_3, shifted from the analogous bands on the bulk species (spectrum e), in agreement with published spectra for this system [20]. However, we suggest that the Mo species associated with poisoning the ceria surface is not observed and that it is only the excess MoO_x that is observable, and only at higher coverages.

4. Discussion

It appears that Mo affects ceria by preventing the reduction of the ceria surface. This conclusion is consistent with the CO–O_2 pulse data, which indicated that higher temperatures were required to add and remove oxygen from the Mo-poisoned surface. This conclusion is also consistent with the observation that there is no carbonate formation on the poisoned surface. Like La_2O_3, Ce_2O_3 is capable of forming a stable carbonate by adsorption of CO_2, while no carbonate is formed on CeO_2 [7]. Assuming that the redox mechanism proposed for the WGS reaction on Pd/ceria is valid [6,7,21], one should expect a change in the reducibility of the ceria surface to severely affect the reaction rate. A key step in the

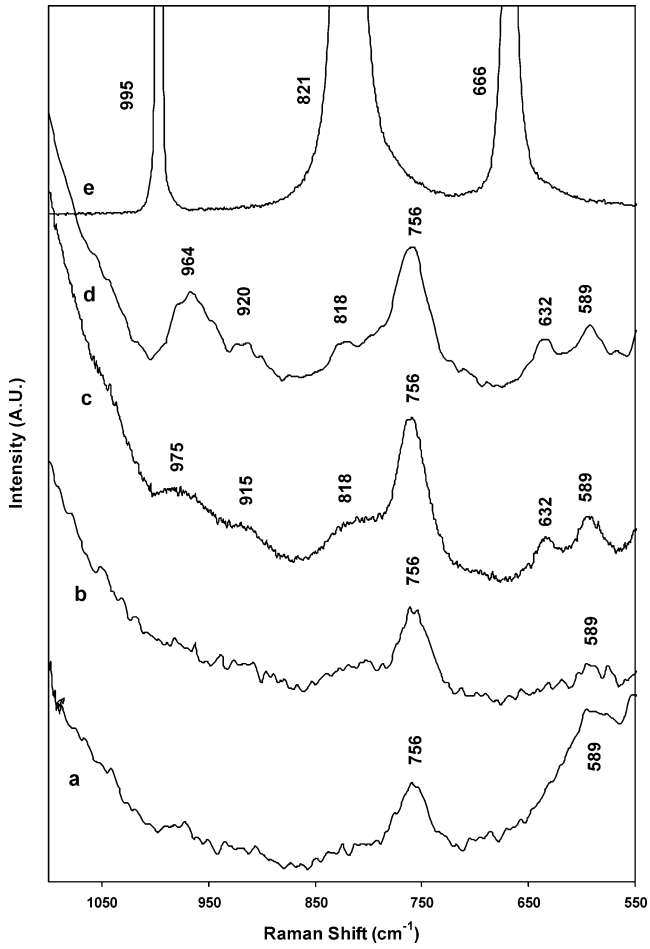

Fig. 7. Raman spectra of (a) ceria, (b) 1 wt% Mo–ceria, (c) 1.25 wt% Mo–ceria, (d) 4 wt% Mo–ceria, and (e) MoO_3.

redox mechanism is the oxidation by ceria of CO adsorbed on Pd. Anything that blocks this step will poison the catalyst.

The two most interesting aspects of this study are that Mo is such an effective poison for reduction of the ceria surface and that only relatively small quantities of Mo, < 2 Mo/nm^2, are required to poison the surface. In order to rationalize the low coverage of Mo that is required to affect WGS activity, it is useful to compare the value we have found in this study to concentrations of Mo in well-defined systems. The surface concentration of Mo^{6+} for the (100) surface of MoO_3 is 4.9 Mo/nm^2 based on crystallographic information. A similar value was obtained by Dong and Chen for an MoO_3 monolayer on ceria [22]. They estimated that the coverage is 4.8 Mo^{6+}/nm^2, assuming preferential exposure of the (111) surface of CeO_2. Based on these values, the MoO_3 in our study is probably not poisoning the ceria surface by a simple blocking mechanism that makes the ceria surface inaccessible. However, 1.8 Mo/nm^2 is a sufficiently high coverage that, if the Mo^{6+} are evenly dispersed over the ceria surface, most of the surface O^{2-} ions could be associated with a Ce^{4+} that neighbors a Mo^{6+}. Furthermore, the decrease in the amount of oxygen transferred in the CO–O_2 pulse data at 473 K, 90 μmol/g, is very similar to the Mo loading in that experiment, 100 μmol/g. Therefore, if special redox sites exist on the ceria surface, there is sufficient Mo present to block those sites.

Since it is hard to imagine that Mo could influence surface oxygen that was more than a few atomic distances away, the Mo must be very evenly dispersed over the surface. It seems unlikely that a random process could provide the high Mo dispersion, so that Mo must react with specific sites on the ceria surface during impregnation. Indeed, the selective removal of cerium hydroxyls upon the addition of Mo would also argue for the reaction of Mo ions with specific sites. The selective removal of cerium hydroxyls could also explain the 2-propanol adsorption results. One would expect the alcohol to form strong hydrogen bonds with the surface hydroxyls and that the decreased reaction of 2-propanol simply follows the removal of these hydroxyls. The mechanism for dehydration of the alcohol is associated with the Lewis acidity of the ceria surface and is probably similar to that observed in a previous study of ethanol on TiO_2 [23].

An even bigger question regards how the presence of Mo ions on the surface affects the surface reducibility. One obvious difference between Mo^{6+} and Ce^{4+} is the charge of the ion. It is tempting to suggest that the more positive ion withdraws charge from Ce^{4+}, making the Ce–O bond stronger. An alternative attempt to explain the effect of Mo is based on the bulk heats of formation for MoO_3 and CeO_2. However, the standard heat of reaction for CeO_2 to Ce metal is 487 kJ/mol of oxygen atoms, while the enthalpy change for reducing MoO_3 to Mo is 250 kJ/mol of oxygen atoms, implying that O^{2-} are bound less tightly to Mo^{6+} than to Ce^{4+}. Both cerium and molybdenum have suboxides that could change this thermodynamic picture. However, standard enthalpy changes for reducing CeO_2 are typically larger. The heat of oxidation for Ce_2O_3 to CeO_2 is 380 kJ/mol of oxygen atoms and this number is reported to be similar for other suboxides on an oxygen atom basis [24,25]. It should also be noted that the reducibility of high-temperature forms of ceria may not accurately describe the reducibility of catalytically active forms of ceria [26].

All of this discussion has assumed that one can treat the properties of Pd and ceria separately. However, there is evidence that specific interactions between the precious metal and the ceria could be important in determining the ease of oxygen transfer between these two components. For example, in model studies of Rh and Pd particles on reduced ceria [27], CO dissociation occurred rapidly on the Rh particles below 400 K, desorbing as CO at 650 K, but only after exchange of oxygen with the ceria. No similar exchange was observed with Pd. More recently, Wang and Gorte reported large enhancements in the WGS activity of Pd/ceria catalysts that had Fe incorporated into the surface [16]. Surprisingly, we find that the addition of Fe causes no enhancement for Pt-based catalysts [28]. Therefore, a complete understanding of the effects of Mo in the present study may require an understanding of how Mo modifies the interactions between Pd and ceria.

Finally, the initial interest in the WGS reaction in our laboratory came from our desire to understand oxygen storage capacity (OSC) in three-way automotive catalysts [11]. In that early work, it was found that the processes that lead to deactivation of OSC also lead to deactivation of WGS activity [6]. The data from a wide variety of model studies suggested that the exchangeable oxygen in ceria and ceria–zirconia mixtures was associated with defects or some other form of meta-stable ceria [29]. From this vantage point, surface Mo may either quench these special sites or prevent this oxygen from migrating to the surface.

Perhaps the most important message from the present study is that ceria-based catalysts exhibit interesting WGS properties that can be greatly modified by processing conditions and the addition of surface dopants. While the present study focused on a dopant that poisoned catalytic activity, we believe the insights gained in this work may lead to new approaches that enhance reactivity.

5. Conclusions

The addition of small amount of Mo (< 2 Mo/nm^2 on ceria) poisons the catalytic activity of Pd/ceria in a WGS reaction significantly. Our study shows that Mo affects the activity by blocking the surface redox ability of ceria. This work provides additional evidence for the redox mechanism of the WGS reaction over Pd/ceria.

Acknowledgment

This work was supported by the DOE, Basic Energy Sciences, Grant DE-FG03-85-13350.

References

[1] A.F. Ghenciu, Curr. Opin. Solid State Mater. Sci. 6 (2002) 389.
[2] J.R. Ladebeck, J.P. Wagner, in: Handbook of Fuel Cell Technology, Wiley, New York, 2003, Chap. 17, in press.
[3] S.L. Swartz, M.M. Seabaugh, C.T. Holt, W.J. Dawson, Fuel Cell Bull. 4 (2001) 7.
[4] J.M. Zalc, V. Sokolovskii, D.G. Loffler, J. Catal. 206 (2002) 167.
[5] X. Wang, R.J. Gorte, J.P. Wagner, J. Catal. 212 (2002) 225.
[6] T. Bunluesin, R.J. Gorte, G.W. Graham, Appl. Catal. B 15 (1998) 107.
[7] S. Hilaire, X. Wang, T. Luo, R.J. Gorte, J. Wagner, Appl. Catal. A 215 (2001) 271.
[8] G.S. Zafiris, R.J. Gorte, J. Catal. 139 (1993) 561.
[9] G.S. Zafiris, R.J. Gorte, J. Catal. 143 (1993) 86.
[10] M.Y. Smirnov, G.W. Graham, Catal. Lett. 72 (2001) 39.
[11] T. Bunluesin, R.J. Gorte, G.W. Graham, Appl. Catal. B 14 (1997) 105.
[12] H. Cordatos, T. Bunluesin, J. Stubenrauch, J.M. Vohs, R.J. Gorte, J. Phys. Chem. 100 (1996) 785.
[13] J. Stubenrauch, J.M. Vohs, J. Catal. 159 (1996) 50.
[14] R.M. Ferrizz, T. Egami, J.M. Vohs, Surf. Sci. 465 (2000) 127.
[15] M. Shelef, G.W. Graham, R.W. McCabe, in: A. Trovarelli (Ed.), Catalysis by Ceria and Related Materials, Imperial College Press, London, 2002, p. 343.
[16] X. Wang, R.J. Gorte, Appl. Catal. A 247 (2003) 157.
[17] A.I. Biaglow, R.J. Gorte, S. Srinivasan, A.K. Datye, Catal. Lett. 13 (1992) 313.
[18] S. Sharma, S. Hilaire, J.M. Vohs, R.J. Gorte, H.-W. Jen, J. Catal. 190 (2000) 199.
[19] A. Laachir, V. Perrichon, A. Badri, J. Lamotte, E. Catherine, J.-C. Lavalley, J. El Fallah, L. Hilaire, F. Le Normand, E. Quemere, G.N. Saurion, O. Touret, J. Chem. Soc., Faraday Trans. 87 (1991) 1601.
[20] X. Du, L. Dong, C. Li, Y. Liang, Y. Chen, Langmuir 15 (1999) 1693.
[21] T. Luo, R.J. Gorte, Catal. Lett. 85 (2003) 139.
[22] L. Dong, Y. Chen, J. Chem. Soc., Faraday Trans. 92 (1996) 4589.
[23] L. Gamble, L.S. Jung, C.T. Campbell, Surf. Sci. 348 (1996) 1.
[24] D.A.R. Kay, W.G. Wilson, V.J. Jalan, J. Alloys Comp. 192 (1993) 11.
[25] M. Mogensen, in: A. Trovarelli (Ed.), Catalysis by Ceria and Related Materials, Imperial College Press, London, 2002, p. 459.
[26] L. Yang, O. Kresnawahjuesa, R.J. Gorte, Catal. Lett. 72 (2001) 33.
[27] E.S. Putna, R.J. Gorte, J.M. Vohs, G.W. Graham, J. Catal. 178 (1998) 598.
[28] T. Luo, S. Zhao, R.J. Gorte, to be published.
[29] E. Mamontov, T. Egami, J. Phys. Chem. B 104 (2000) 11110.